THE USE OF A DEEP HONEYCOMB TO ACHIEVE HIGH FLOW QUALITY IN THE ARA 9' x 8' TRANSONIC WIND TUNNEL

J E Green, C A McHugh, A J Baxendale, D R Stanniland
Aircraft Research Association Ltd,
Manton Lane, Bedford MK41 7PF, England

SUMMARY

Until August 1990, the 9' x 8' Transonic Wind Tunnel at ARA Bedford relied on a single gauze screen, in combination with a relatively high contraction ratio, to achieve flow uniformity in the test section. This screen has now been replaced by a honeycomb with a high ratio of cell length to diameter. The paper sets out the reasons for the change, outlines the aerodynamic investigations that preceded it, describes the main features of interest in the honeycomb construction and reports the resulting changes in tunnel flow quality. Detailed surveys of total pressure, flow direction and turbulence show that a high degree of flow uniformity has been achieved across the whole of the test section, with unsteady velocity components of 0.1% longitudinally and 0.2% laterally. Mean flow velocity and direction is close to that which would be obtained with completely uniform reservoir conditions and has remained unchanged since the honeycomb was installed. Further work will be required, however, to determine the relative magnitudes of the convected (turbulent) and radiated (acoustic) components of the velocity fluctuations.

INTRODUCTION

The 9' x 8' Transonic Wind Tunnel (TWT) at ARA Bedford was opened 36 years ago, in May 1956, and began commercial operation in the spring of the following year. As Fig 1 shows, it is a closed-return tunnel of conventional design. It has perforated test section walls downstream of a flexible nozzle, giving a Mach number range from zero to 1.4. Motive power is a two-stage fan driven by a 25000 hp motor, supplemented at the higher Mach numbers by plenum chamber suction driven by a 13000 hp compressor. There have been no significant aerodynamic changes to the tunnel since operations began, other than the fitting of vortex generators in one corner of the first diffuser to improve flow steadiness during half model testing.

The fan is conventionally situated immediately after the second corner. Downstream of the fan there is a long diffuser of 6° included angle, followed by a rapid diffuser in which the cross section changes from octagonal to rectangular at the cooler face. The cooler, which consists of banks of vertical, finned, water cooled tubes, is at the point of maximum cross section area in the tunnel (16.7 times the test section area) and was designed to have a pressure drop across it of 3.5 times local q. Downstream of the cooler there is a 30 per cent reduction in area combined with a reversion from rectangular to octagonal cross section. Thereafter, the cross section remains constant through the third corner, cross leg and fourth corner into the settling chamber. The turning vanes in these two corners are of sheet metal and are of 10in chord and 2.5in pitch. The contraction ratio from settling chamber to test section is 11.3.

The tunnel was designed with a single gauze screen in the settling chamber to provide flow smoothing. This, in combination with the high contraction ratio and the gross levelling of total pressure by the 3.5q pressure drop in the cooler, produced a highly uniform total head in the test section. Uniformity of flow direction was also good and turbulence levels low, enabling ARA to develop test techniques which give the high degree of accuracy and repeatability now required for transport aircraft performance testing.

The settling chamber cross section is a regular octagon, 31.3 ft across flats, and the screen was designed to take up a paraboloidal form, dished 4ft on its axis, under wind load. The screen was made of high tensile phosphor bronze wire, 30 mesh x 34 swg, giving a 2q pressure drop at typical tunnel conditions. Before installation it was pre-formed into its paraboloidal shape by stretching over formers and its edges were hemmed in the shape of the intersection between the

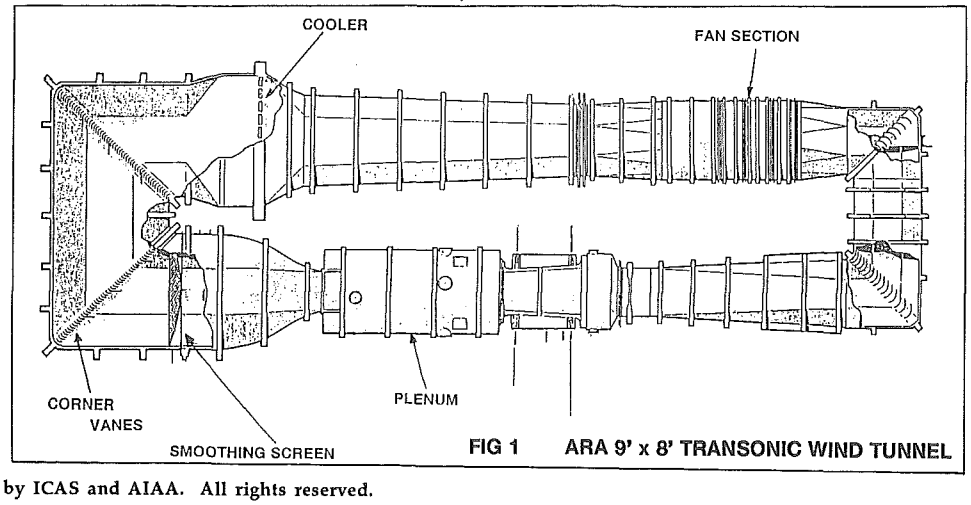

FIG 1 ARA 9' x 8' TRANSONIC WIND TUNNEL

paraboloid and the octagonal tunnel shell. The total axial wind load on the screen, when the stagnation presssure was 1.2 bar and the pressure drop across the screen had been increased by 50% by the build up of dirt, was estimated to be approximately 11000 lb, giving as a design load a tension of some 250 lb per ft run at the periphery of the screen.

The mounting of the screen to the tunnel shell is shown in Fig 2. The edges of the screen were held between sheets of 1/8 in thick rubber clamped by a steel strip measuring 0.375in x 2in to a mounting plate fixed to the tunnel shell. The mounting was hidden from the airflow by a shallow streamlined blister. The screen had double thickness "dragons teeth" reinforcement sewn around its edges and was installed with its weft and warp at 45° to the vertical. If the wind load was uniformly distributed around the periphery, the calculated tension in the wire of the gauze was a factor of 5 down on the yield of the wire.

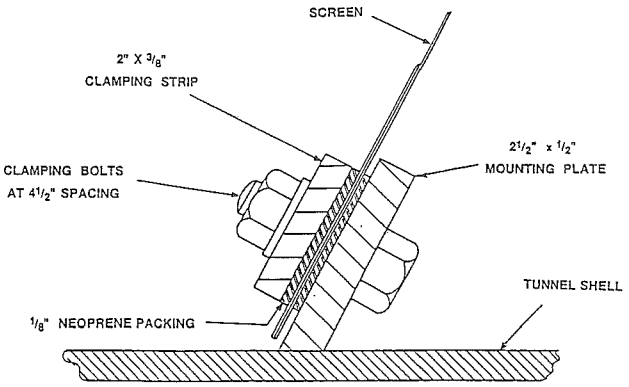

FIG 2 SCREEN EDGE FIXATION

During the life of the tunnel the screen was replaced a number of times. Invariably, after prolonged use, small splits developed in the screen. In the early stages of deterioration these were repaired by stitching but, in due course, it became necessary to make and install a new screen. During the 1980s the tunnel had a fairly heavy workload and the life of the screen was approximately four years. The process of removing the existing screen and installing a new one, which required the erection of scaffolding in the settling chamber on each side of the screen, put the tunnel out of action for two weeks approximately.

It was the appearance of the first splits in the tunnel's last screen, in the spring of 1989, which began the process that ended with the installation of a honeycomb. At that time the screen was some 3 years old and the splits had appeared sooner than expected. While laying plans to make and install a replacement screen, ARA engineers also asked themselves why the screen had a relatively short life and what might be done to increase it. Although the heavy tunnel workload since the last screen was installed was accepted as the primary reason for its early deterioration, it also became apparent that some of the wires in the screen were more highly loaded than had been assumed in the stressing calculations. From consultation with textile experts it was learned that, because a woven fabric is very much stiffer in tension along axes aligned with the fibres than along axes oblique to the fibres, the assumption that the wind load on the screen is carried uniformly along its periphery was in error. In fact, the screen deformed under wind load in such a way that the load was carried almost entirely by the orthogonal bands of fibre which pass through the central part of the screen, as sketched in Fig 3. For the ARA TWT, with the weft and warp aligned at 45° to the vertical, this meant that the wind load was carried by the edges of the screen attached to the sloping walls of the tunnel, leaving the edges attached to the horizontal and vertical walls virtually unloaded. By this process, the load per unit length of periphery was approximately doubled on the sloping walls of the tunnel.

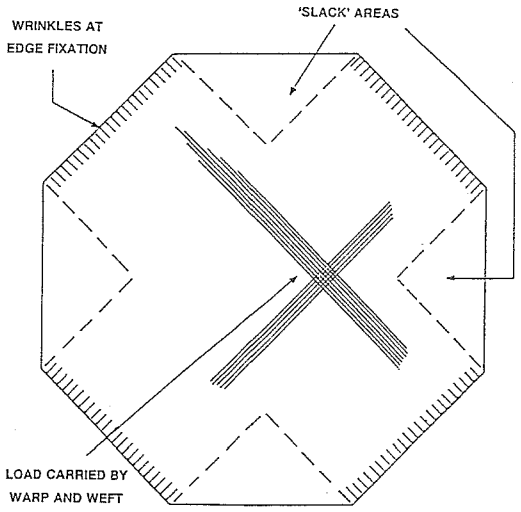

FIG 3 UNEVENNESS IN TENSION AT SCREEN EDGES

The maldistribution of stress in the screen was exacerbated by distortion of the screen around the holes through which the clamping bolts passed. The holes were of 0.5in diameter, spaced at 4.5in intervals, and were punched in the screen during its fitting into the tunnel. It was observed that, over a period of time, the fibres in line with the holes pulled through the clamping rubber sufficiently to transfer their load to adjacent fibres. Eventually the screen took on a wrinkled appearance along its diagonal edges, by which time the loads in the most highly stressed fibres were of the order of four times the loads calculated when the screen was stressed. The design safety factor was thus largely eroded and individual wires began to fail, creating load concentrations which caused adjacent wires to fail and small circumferential splits to form. The process was a slow one but inexorable. The growth of an individual split could be arrested by stitching but in due course new splits would form and the process would continue.

In the face of this fundamental weakness in the screen design, a search began for a robust alternative which would be at least as good aerodynamically but which would have a service life appreciably greater than the existing design. The RAE 5m pressurised low speed tunnel, which entered service two decades after the ARA TWT, has a screen of

similar size carrying comparable wind loads. However, the two design weaknesses of the ARA screen have been avoided. Holes for clamping bolts have been pierced with a spike rather than punched, the holes are more closely spaced and, most importantly, the edges of the screen are attached to spring-loaded bars which maintain an even tension around the periphery. The screen is also of heavier gauge wire and has a higher design safety factor than the ARA screen.

Spring-loading the edges of the screen requires a mounting system outside the air swept surface of the settling chamber and this was not thought practicable in the TWT. A wide range of alternative ways of reducing the peak stresses in the screen was therefore considered. The simplest solution would have been to use a screen of coarser mesh, with heavier gauge wire and possibly a greater open area ratio. However, to achieve a substantial increase in screen life would have required an appreciable increase in screen coarseness and, with it, a possible degradation in tunnel flow quality. As alternatives to strengthening the screen, various methods of providing support for it over its central area were considered. One of these was to build up a load-carrying honeycomb downstream of the screen and allow the screen simply to rest against its upstream face.

In such an arrangement, the screen was conceived as providing the pressure drop to reduce non uniformities in total pressure while the honeycomb provided mechanical support for the screen. A conventional wind tunnel honeycomb was envisaged, with a cell length to diameter ratio in the region of 6 to 8. In addition to supporting the screen, the honeycomb would reduce residual streamwise vorticity and the lateral turbulent velocity components. Its drawback would be the absence of a screen downstream, which is usually installed to reduce the turbulence and non uniformity of total pressure created by the wakes of the honeycomb and its supporting structure.

A DEEP HONEYCOMB AS AN ALTERNATIVE TO A SCREEN

It was the assessment of the residual disturbances at the outlet of a honeycomb, at the physical scales practicable in the TWT, that led to the idea of replacing the screen with a deep honeycomb.

The rationale for such a course of action is set out by Lumley and McMahon[1], who present a theoretical treatment of a honeycomb as a means of reducing turbulence and report its successful application to the large water tunnel at the Ordnance Research Laboratory. These authors claim two important advantages for a honeycomb over a screen in reducing turbulence: (a) the annihilation of transverse fluctuations (provided the cell L/D is sufficiently high to give fully developed pipe flow); (b) the inertial effect of the mass of fluid in a cell in reducing longitudinal fluctuations. These advantages are offset, however, by the turbulence created by the honeycomb itself. A low turbulence level in the test section will be achieved only if this self-generated turbulence is of small scale, so that it decays rapidly during its passage from settling chamber to test section.

The pressure drop through a deep honeycomb arises from the skin friction in the pipe flow in each cell. It is Reynolds number dependent and is approximately proportional to the ratio of cell length to effective diameter. For a given pressure drop coefficient k ($= \Delta p / \frac{1}{2} u_\infty^2$), the effects of a honeycomb and a screen on non-uniformities in the mean streamwise flow are virtually the same. To first order, both devices reduce spatial variations in streamwise velocity by a factor of 1 + k. They differ however in their effect on transverse velocity components, a screen reducing these by a factor of $(1 + k)^{\frac{1}{2}}$ whilst a deep honeycomb effectively eliminates them.

The further reduction in non-uniformity produced by a contraction is similar in kind to that produced by a screen: streamwise non uniformity u/U is reduced by a factor C, where C is the contraction ratio, whilst flow angularities v/U and w/U are reduced by a factor $C^{\frac{1}{2}}$. For the ARA TWT, with k = 2 and C = 11.3, the theoretical effect of screen and contraction acting together on non-uniformity in the flow out of the 4th corner was to reduce u/U by a factor of 34 but to reduce flow angularity only by a factor of 5.8. The same theoretical arguments apply approximately to the time-dependent flow, the longitudinal components of turbulence being reduced much more than the lateral components by screen and contraction.

From the standpoint that the steady and unsteady transverse velocity components in the test section are arguably the most important measures of tunnel flow quality, it is unfortunate that both screen and contraction are relatively ineffective in reducing them. In this respect a honeycomb and contraction are a much better combination. Their strengths and weaknesses are complementary and together they offer the prospect of eliminating mean vorticity from the flow to leave residual honeycomb turbulence as the most significant factor degrading test section flow quality. This reasoning, and an assessment of the turbulence levels likely to be obtainable in the test section, led to the decision to install a honeycomb as the sole means of flow smoothing in the TWT.

REQUIRED AERODYNAMIC AND STRUCTURAL CHARACTERISTICS

The original TWT screen had a k of 2. In the 1950s and 60s this was a widely used norm in wind tunnel design, deriving in part from pre-war work which purported to show that a 2q screen totally eliminated flow non-uniformities. Although Taylor and Bachelor had shown in 1949[2] that this analysis was in error, it was not until the 1960s, following work by Bradshaw on non-uniformities in tunnel boundary layers, that the use of more open screens, usually two or more in series, became common.

For the TWT, the existing 2q screen, in combination with the high contraction ratio, had produced a high degree of uniformity of total pressure in the test section. The screen pressure drop accounted for approximately 2% of the tunnel drive power. With this balance between cost and benefit, there seemed no strong case for aiming for a pressure drop across the honeycomb any greater or less than 2q.

The design targets initially set for the honeycomb were therefore:

1 Cell L/D chosen to produce an overall pressure drop of $2q_\infty$ at normal operating Reynolds numbers;

2 L sufficient for the honeycomb to be structurally stable;

3 D to be as small a practicable, consistent with 1 and 2 and with 'cleanability' requirements;

4 Prefabricated, modular construction to minimise tunnel down time for installation;

5 Test section turbulence level ~ 0.1%.

Because there was to be no screen downstream of the honeycomb it was decided, in the interests of uniformity of flow quality, to construct a honeycomb which was essentially seamless - ie, not to construct it as a structural egg-box housing blocks of honeycomb material. This decision, together with criteria 1-3, effectively sized the honeycomb cells, giving values of D and L of the order of 1in and 70in respectively. A search for commercially available honeycomb material of these proportions proved fruitless, however, and so the final characteristic defined for the honeycomb was that it should be built from other components which could be obtained readily and at reasonably short notice.

PRELIMINARY INVESTIGATION OF ALTERNATIVE CONFIGURATIONS

Several alternative forms of honeycomb construction were considered and three samples of honeycomb were built and tested aerodynamically. The geometric characteristics of these are shown in Fig 4.

Building a honeycomb as a stack of horizontal tubes was the first option to be investigated. Because tube wall thickness was expected to have a significant effect on the self-generated turbulence downstream of the honeycomb, two samples of honeycomb were constructed using tube of the same external diameter but appreciably different wall thickness. The samples were built by laying the tubes in a jig and bonding them along their contact lines. The sample with the thinner wall was tested with the interstitial gaps between the tubes both open and plugged. This was done because these gaps were thought likely to become blocked with dirt over the life of the honeycomb, and it was considered preferable to achieve consistent behaviour by sealing them at the outset, provided that any resulting increase in turbulence level was not excessive.

The third sample of honeycomb tested was made of a combination of corrugated and flat sheet aluminium. The corrugated sheet was manufactured as roofing material. Many different profiles of sheet were on the market but only one was found which, when sheets were laid back to back, produced cells which were regular hexagons. This came in one size only, which gave too large a value of D to meet the

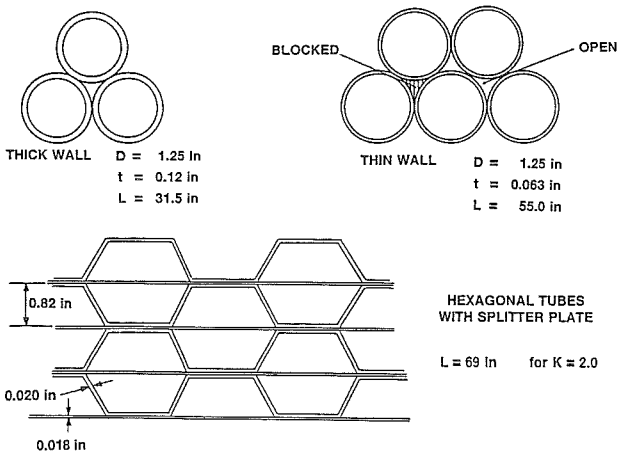

FIG 4 ALTERNATIVE 2q HONEYCOMBS

design aims: space limitations in the settling chamber restricted L/D and would prevent the required pressure drop being achieved, while the larger scale turbulence would decay more slowly and result in higher than desired turbulence levels in the test section. To circumvent this problem, thin horizontal splitter plates were introduced between each layer of corrugations. These served two purposes, to reduce the effective D to an acceptable value and to produce a design of module which could resist collapse under the weight of the honeycomb above it without the support of a containment wall at the side.

The samples of honeycomb made for aerodynamic test were 1 ft high, 4 ft wide and of a length predicted to give a 2q pressure drop. They were tested in the boundary layer tunnel at RAE Bedford[3] with the tunnel configured as a 1 ft high, parallel-walled channel. Pressure drop across the honeycomb was measured as a function of flow velocity (ie Reynolds number) and hot-wire anemometer traverses were made at several positions over a range of streamwise distance from 14 in to 86 in downstream of the honeycomb.

Fig 5 shows the variation of pressure drop with flow velocity for the three samples. Although the limitations of the theory used to determine the length of the samples are evident from

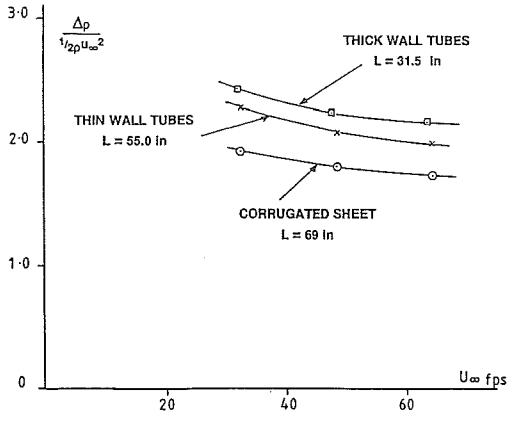

FIG 5 PRESSURE DROP COEFFICIENTS OF SAMPLES

this figure, each sample gave a pressure drop of approximately 2q. This was more than sufficient to ensure that fully developed turbulent pipe flow was obtained within the length of a cell, so that the characteristics of the self-generated turbulence measured downstream of the honeycomb would be independent of the length of the sample and the pressure drop across it.

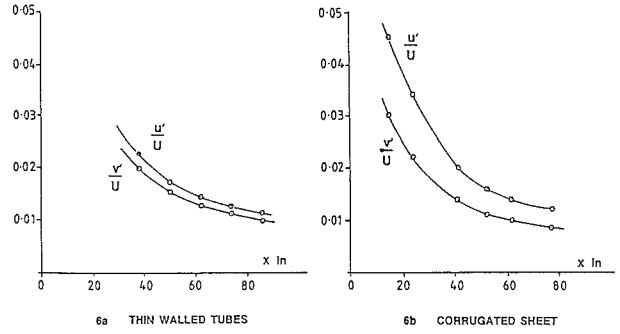

FIG 6 LONGITUDINAL & LATERAL TURBULENT INTENSITIES

Fig 6 shows the streamwise variation of the longitudinal and lateral turbulent intensities downstream of the thin walled tube sample (6a) and the sheet aluminium honeycomb (6b) at a mean flow velocity of 50 ft/sec. In Fig 7 the inverse square of the intensities is plotted against distance downstream from the honeycomb for all three samples. Longitudinal components are shown in Fig 7a and lateral components in Fig 7b. The linear variation with distance is similar to that observed with grid-generated turbulence and extrapolation of the lines provides a good starting point for estimating turbulence in the working section. The tube diameter (1.25 in) has been used for convenience to scale streamwise distance for all three samples, though the initial scale of the big eddies will not be the same for the three samples.

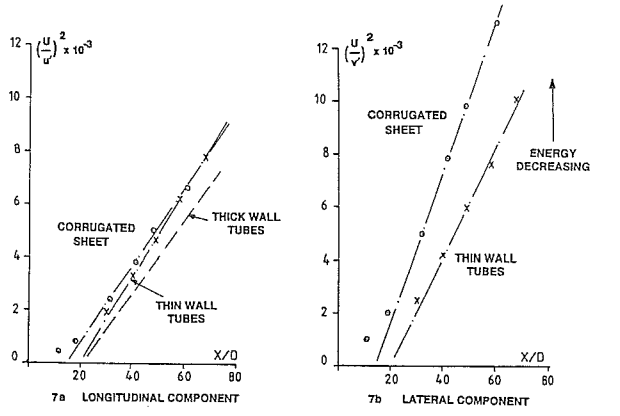

FIG 7 STREAMWISE DECAY OF TURBULENT ENERGY

It may be noted from Figs 6 and 7 that, although the longitudinal turbulence intensities are approximately the same for the thin tube and the aluminium sheet samples, the latter generates appreciably less intense transverse fluctuations than the tube. Moreover, the ratio of almost 2 between the energies of the longitudinal and lateral fluctuations behind the aluminium sheet sample persists over the full range of x. The reason for this difference is thought to be a more vigorous mixing process downstream of the tubular honeycomb, caused by the greater base area of the tubes and the low energy efflux from the interstitial passages.

For the thick walled tube only longitudinal turbulence was measured (Fig 7a). The energy in this was approximately 25% higher than for the thin walled tube, which is less than might have been expected from considering the relative levels of mean dynamic pressure or turbulent stresses within the two tubes. The effect of blocking the interstitial gaps on the thin walled sample, not shown in the figures, was relatively small: overall pressure drop was increased by 9%, longitudinal turbulence was not measurably changed whilst the energy in the lateral components was increased by between 4 and 8%.

Some measurements were made of the effect of the thin tube and aluminium sheet samples on turbulence generated by the coarse grid of 4 in x 2 in timber sketched in Fig 8. The grid was placed in the constant area section of the tunnel at a position 40 in upstream of the front face of the honeycomb. Hot wire traverses were made at a position approximately midway between the generator and the honeycomb and at a number of stations downstream of the honeycomb.

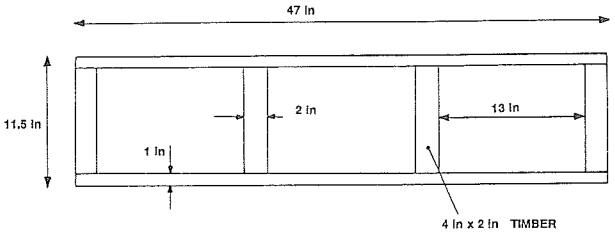

FIG 8 TURBULENCE GENERATOR

The grid produced turbulence intensities u'/U at the upstream measuring station which varied from 3% to 10% over the height of the duct, the spectrum being characterised by a high peak in energy at approximately 85 Hz as illustrated in Fig 9a. The figure, which refers to the thin walled tube honeycomb, shows this energy to be substantially reduced by the honeycomb except at frequencies below 20 Hz. Comparisons of wide band spectra downstream of the honeycomb with and without the turbulence generator in place show no perceptible effect of the generator except at the very lowest frequencies. Fig 9b shows turbulence intensities measured downstream of the corrugated sheet honeycomb with and without the generator in place. The increase in lateral turbulence is small. The much greater increase in longitudinal turbulence is found, from the differences in $(u'/U)^2$ with and without the generator, to be independent of distance downstream and to correspond to

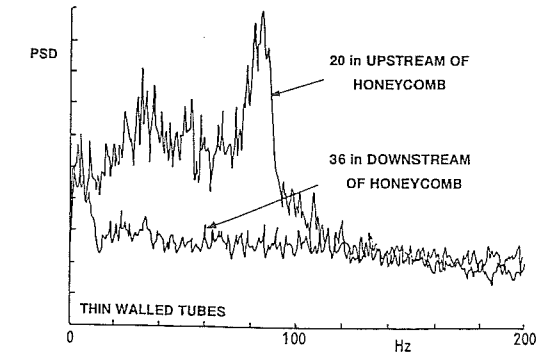

FIG 9a LOW FREQUENCY PSD OF LONGITUDINAL COMPONENT WITH TURBULENCE GENERATOR IN POSITON

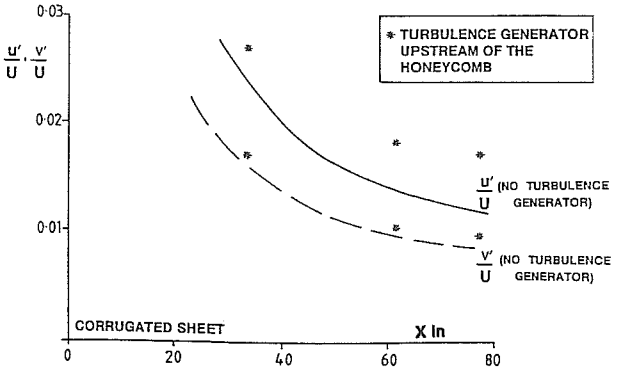

FIG 9b INCREASE IN TURBULENCE INTENSITIES

FIG 9 EFFECT OF A TURBULENCE GENERATOR UPSTREAM OF HONEYCOMB

an intensity u'/U of approximately 1.2%. This represents the residue of the low frequency component of the incident grid turbulence, which has a wavelength many times the cell diameter. It thus has the character more of a pulsating than an eddying flow and, from Fig 9b, it is evident that it has only a very weak tendency to transfer its energy into lateral motion.

The conclusion of these various investigations was that aluminium sheet construction was to be preferred aerodynamically to circular tubes because it produced significantly less intense transverse velocity fluctuations. The space available in the settling chamber would limit the length of the honeycomb, so that a value of k of only slightly more than 1.5 would be achieved at normal operating conditions. This was not considered a serious drawback however because of the large contraction ratio into the test section. Considerations of weight, the availability of suitable material and the practicalities of manufacturing the honeycomb in modular form also favoured the sheet metal construction. The decision was therefore made to build a honeycomb of the cross section shown in Fig 4 and having a depth of 59in.

CONSTRUCTION

The corrugated sheet was available in a standard width of 44.3in, which gave exactly 15 wavelengths of the corrugation. For ease of handling during the final assembly, the standard honeycomb module was made of four layers of corrugated sheet and four layers of flat sheet joined together as shown in Fig 10. This produced a module measuring 44.3in x 59in x 3.3in and weighing about 40 lb, which could be easily carried and manoeuvred into position by two people.

The modules were made by bonding the sheets together, using an epoxy resin adhesive, in a compression jig which turned out modules of uniform width and height. For a standard module, each layer was bonded to the one above at three points close to each end of the module, as shown in Fig 10. When the adhesive had set, the module was removed from the jig and the sheets were spot welded together close to the adhesive bond. In the assessment of honeycomb strength, loads were assumed to be carried entirely by the spot welds.

The joint pattern shown in Fig 10 produced a module which was very stiff in most directions but quite flexible in bending about a longitudinal axis. As a result, under the weight of the layers above, a module deformed readily to take up any irregularity in shape in the layer below and unwanted horizontal gaps in the honeycomb were avoided. In parts of the honeycomb where load concentrations occurred the number of spot welded joints was increased, approximately one fifth of all modules being made with all joints spot welded.

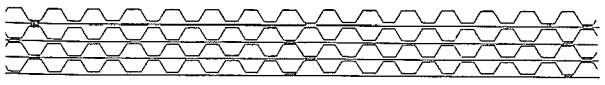

12 GLUED AND SPOT WELDED JOINTS AT EACH END OF MODULE, PATTERNED AS SHOWN

FIG 10 JOINT PATTERN FOR STANDARD MODULE

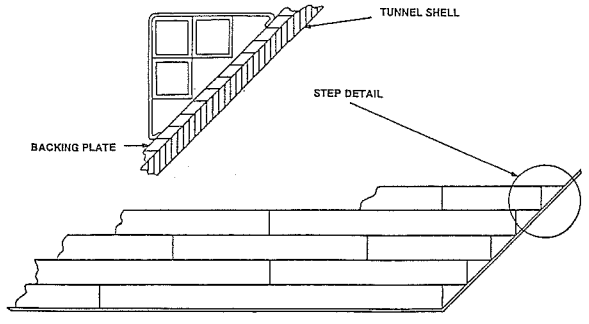

FIG 11 BONDING OF MODULES

The honeycomb was constructed by laying the modules in the pattern shown in Fig 11, with the break between two modules in one layer lying beneath the centre line of a module in the layer above. In bricklaying terms, this pattern is known as "stretcher bond" and is widely used in wall building. It proved a very effective means of compensating

for a small irregularity which was found consistently in the profile of the corrugated sheet and which resulted in all modules being thicker in the centre than at the sides. As each module was laid, it was bonded front and rear to the module below, at approximately ¼ and ¾ span, by a slow curing rubber adhesive. This was done in preference to relying on friction between modules to prevent internal movement in the honeycomb under cyclic aerodynamic and thermal loads.

To enable the weight of the side portions of the honeycomb to be carried by the sloping walls of the settling chamber, a staircase was mounted on the tunnel wall as shown inset in Fig 11. The steps, which were the same height as the modules, were made of sheet aluminium reinforced by square section to produce similar aerodynamic characteristics to the honeycomb itself.

Because aluminium has a greater coefficient of expansion than steel, the honeycomb will expand relative to the tunnel shell as the tunnel warms up to its normal operating temperature. The honeycomb was therefore built to stand free of the tunnel sidewalls and roof, the gap being sufficient to avoid the honeycomb imposing any substantial loads on the tunnel shell in the event of a failure of the tunnel temperature control.

Embedded within the honeycomb are four horizontal beams made of 0.08 in aluminium sheet and having the same span and chord as the honeycomb. Each beam is separated from the ridges of the honeycomb above and below by thin strips of rubber which run the full length of every ridge and are bonded adhesively to both ridge and beam. The role of the beams, in the original design concept, was to transfer the aerodynamic load on the honeycomb to the tunnel structure, the beams being anchored by tie rods at their ends and mid points to the tunnel shell and to a central support upstream of the honeycomb. The location of the beams is shown in front elevation in Fig 12a and the central support is shown in the side elevation of the settling chamber in Fig 12b. The central support is a steel beam, 5/8in x 18in, suspended from the roof of the tunnel and anchored against the honeycomb loads by diagonal links attached to the tunnel shell close to the heavy frame forming the fourth corner. The points of attachment of the links to the central support were chosen so as to minimise the deflections of the anchor points of the horizontal beams, thereby minimising deflections of the honeycomb itself. Tie rods connect the horizontal beams to the central suport and, at the sides, to short arms welded to the tunnel shell. The central support is stabilised by lateral tie rods. Flow surveys immediately after installation showed evidence of a faint shadow from the central support and this was reduced by enclosing it in an aerodynamic fairing.

After more than a year of service, it was found during a routine inspection that the block of honeycomb between the second and third beams had moved 15 mm downstream at its port edge, giving it a slew of 0.1° relative to the rest of the honeycomb. The movement was monitored during a tunnel run and it was found to be shifting at approximately 0.04 in per hour, an indication that the fault had developed only

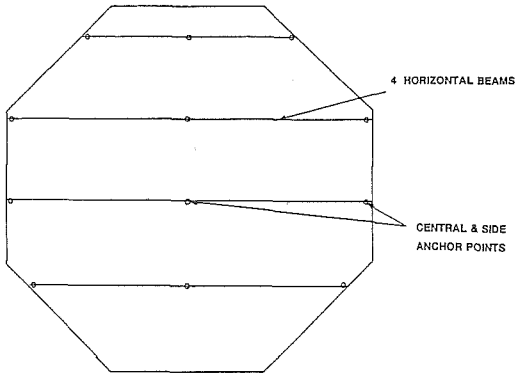

FIG 12a ORIGINAL METHOD OF REACTING AERODYNAMIC LOAD (FRONT)

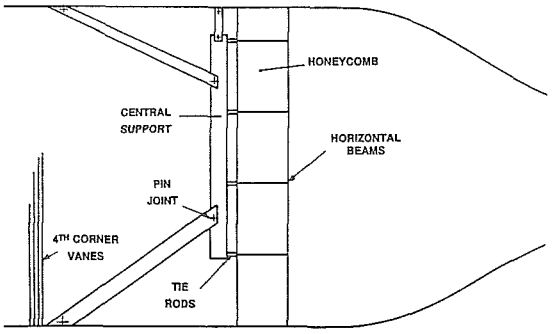

FIG 12b ORIGINAL METHOD OF REACTING AERODYNAMIC LOAD (SIDE)

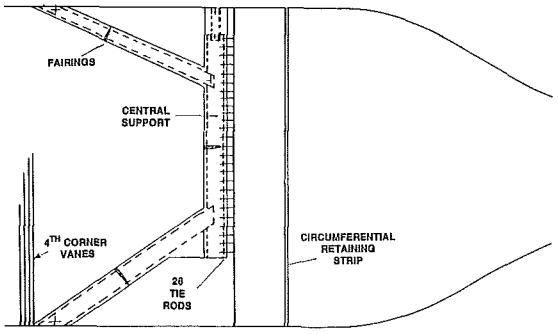

FIG 13 REVISED METHOD OF REACTING AERODYNAMIC LOAD (SIDE)

recently and that urgent corrective action was needed. Further investigation revealed that the adhesive between the rubber strips and the honeycomb had become viscous as a result of migration of plasticiser from the rubber into the adhesive. The deterioration was progressive but eventually creep could be expected to begin at every interface between honeycomb and beam. A new method of reacting the aerodynamic load was therefore devised and is illustrated in Fig 13. The tie rods to the four beams have been disconnected so that the beams no longer transmit any load. The honeycomb is now restrained at its downstream edges

by shallow circumferential stops on the sloping and vertical walls of the settling chamber. Load is transmitted to the central support by a vertical line of 26 adjustable tie rods which are attached to slender spears, each passing through the honeycomb and hooking over the trailing edge of a cell. This form of support spreads the load more evenly through the honeycomb and ensures that the central support can apply only an upstream load to the honeycomb, thereby minimising the cyclic loading arising from differential thermal expansion between the tunnel shell and the central support framework.

Before completing the installation of the new support system, the slewed block of honeycomb was realigned by loading it mechanically and heating the beams electrically to increase the creep rate of the degraded adhesive. The faired central support and the new tie rods are shown in Fig 14.

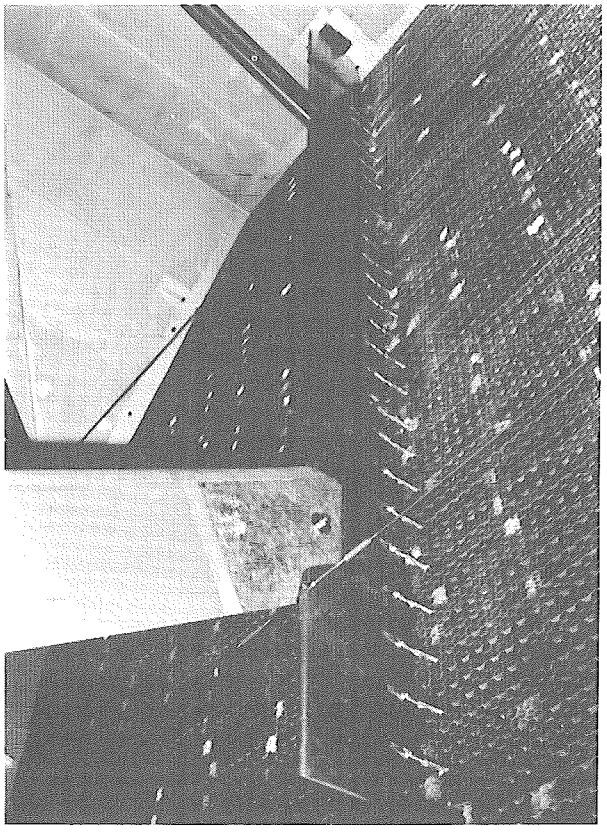

FIG 14 FINAL CONFIGURATION OF CENTRAL SUPPORT

From first thoughts to installation of the honeycomb took approximately a year and a half. The search for a long-term remedy for splits in the screen began early in 1989, the idea of having only a honeycomb crystallised in May of that year and aerodynamic investigations of tubular honeycomb samples were made in June and September. The alternative solution, using aluminium roofing material, had gained favour by November and samples had been made, and tested aerodynamically and structurally by early 1990. An order was placed for 15 tons of aluminium roofing and flat

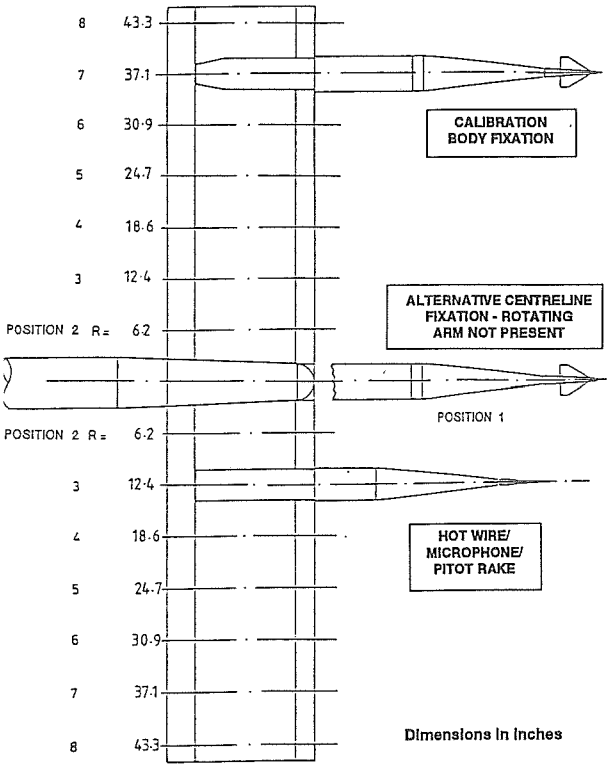

FIG 15 TUNNEL FLOW SURVEY INSTALLATION

sheet material in February, delivery was in March and 900 modules had been manufactured in-house by July. The Transonic Tunnel was closed down for a five week period in August and September 1990, during which time scaffolding was installed in the settling chamber, the screen removed and all traces of its support system removed by flame cutting and grinding, the honeycomb was built, its central support installed, the scaffolding removed and the tunnel cleaned out. The job was carried out by ARA engineering staff working double shifts, 6 am to 11 pm, 7 days per week for the five week period. One factor which extended the timescale was the care needed to align each module precisely. The accuracy of longitudinal alignment in a horizontal plane maintained throughout the erection process was generally ±0.02° on the centre line and the same for the parallelity of adjacent modules. Longitudinal alignment in a vertical plane, which was governed by a set of rails welded to the tunnel floor to provide as level as possible a base for the honeycomb, was also generally to within ±0.02° with a maximum deviation of 0.06°.

The removal of the old screen left the tunnel without any particle catcher other than the grease trap which sits permanently in the lower half of the contraction. A plan has been devised to install a flow cleaning screen which would be placed ahead of the fourth corner and use the corner as its support. This would give an additional 1q pressure drop ahead of the honeycomb and should provide a further slight improvement in flow uniformity and steadiness in the test section. Tunnel cleanliness is monitored continuously, however, and the experience of the 18 months of tunnel operation since the honeycomb was installed is that a satisfactory level of cleanliness is maintained without a cleaning screen.

FLOW QUALITY MEASUREMENTS

Tunnel flow surveys before and after the installation of the honeycomb were made using the purpose built traversing rig shown in Fig 15. This rig, which is mounted from a complete model cart on a standard model sting, can be rolled through 360° to enable a range of measuring instruments to be traversed in a circle at each of the radial positions shown. The rig is designed to give a flow deviation due to aerodynamic interference at the probe positions of less than 0.01°. A calibration body, comprising a cruciform pair of wings and a slender body mounted on a strain-gauge balance, is capable of measuring the local flow angle to 0.01°, giving an overall accuracy of 0.02° in flow angularity. It also measures the unsteady lateral flow angle components at frequencies below 30 Hz. This is above the frequency at which the honeycomb cuts off upstream turbulence, as can be seen in Fig 9a.

Alternative instrumentation fitted to the opposite arm of the rig comprised a pitot rake to survey the stagnation pressure in the test section, a microphone and a crossed hot wire anemometer, each of which was mounted at positions 3, 5 and 7 on the arm (Fig 15). Measurements were also made with the arm removed and the calibration body, microphone or hot wire mounted on the centreline at position 1. In this way a survey of those parts of the tunnel cross section relevant to the testing of complete models and half models was completed.

Additional data were obtained from three strut mounted microphones installed on the starboard wall. The upstream microphone was mounted 20 in above the tunnel centreline, approximately 60 in upstream of the probes on the traversing rig, whilst the two downstream microphones were installed 20 in above and below the tunnel centreline in the plane of the probes on the traversing rig. In a separate set of tunnel runs, turbulence measurements were made in the settling chamber using a crossed hot wire probe positioned 88in downstream of the screen, 34in laterally from the centre line and 61in above the floor.

Measurements carried out prior to the installation of the honeycomb showed essentially the same flow angularity as had been measured using a yawmeter rake in earlier calibrations of the tunnel. In Fig 16, the flow angle vectors at M = 0.8 are plotted in a form which emphasises flow non-uniformity. They show that there is a weak vortex in the lower, starboard quadrant, with still weaker vortices in the adjacent starboard upper and port lower quadrants. Another indication of these vortices is seen in Fig 17, where the low frequency unsteady flow angles measured using the calibration body show corresponding regions of unsteadiness, notably in the lower starboard quadrant of the tunnel.

The improvement in the test section flow angularity due to the installation of the honeycomb is immediately apparent in Fig 18. The flow pattern no longer shows any indication of large scale non-uniformity and is essentially a net outflow associated with a transpiration through the porous walls.

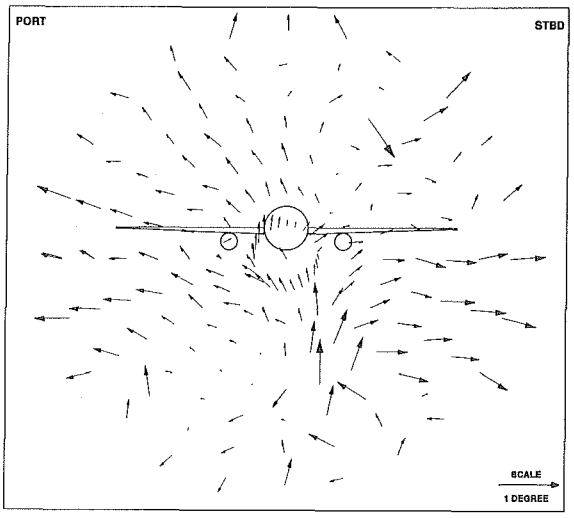

FIG 16 M = 0.8 FLOW ANGLE VECTORS WITH SCREEN

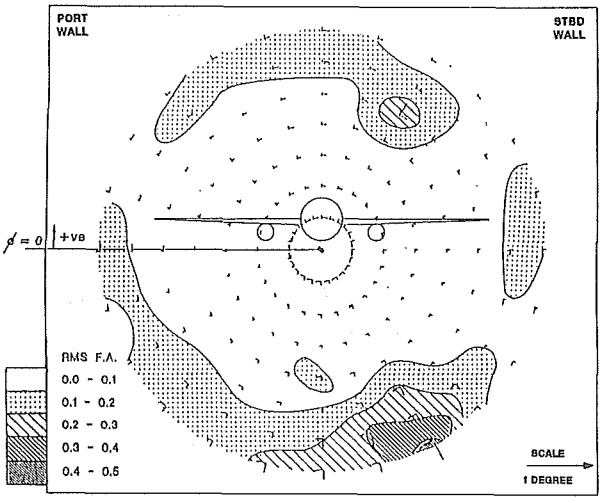

FIG 17 M = 0.8 RMS FLOW ANGLE COMPONENTS WITH SCREEN

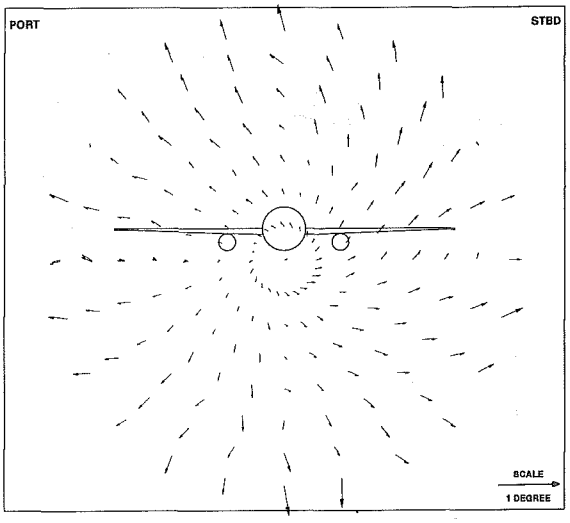

FIG 18 M = 0.8 FLOW ANGLE VECTORS WITH HONEYCOMB

The low frequency unsteady flow angles are not shown here because the RMS flow angle is everywhere less than 0.1° and hence below the level of the first shaded contour in Fig 17.

The flow angle vectors in Figs 16 and 18 have been corrected to allow for the influence of a 0.3° divergence of the tunnel roof which is incorporated to compensate for the growth of the boundary layer on the tunnel walls. A simple model has been developed to predict this effect on the expected flow angle in the tunnel. Fig 19 compares this prediction for a circumferential variation at a radius of 25in with uncorrected measurements obtained before and after the installation of the honeycomb. Installation of the honeycomb has evidently eliminated the weak vortical motion from the original tunnel flow and generated a flow which is close to that which would be produced by ideal reservoir conditions. There is, however, a slight shadow caused by the upstream support strut which is identifiable as a small blip in the flow angle at = 90°, 270° on this radius. This can also be identified as a deficit in the test section stagnation pressure contours, shown in Fig 20. It should be noted, however, that this is only just within measurement accuracy, amounting to a local reduction in H of approximately 0.1 millibars in a reading which is measured to an absolute accuracy of ±0.3 millibars. Hence this is not considered to be significant for normal model testing.

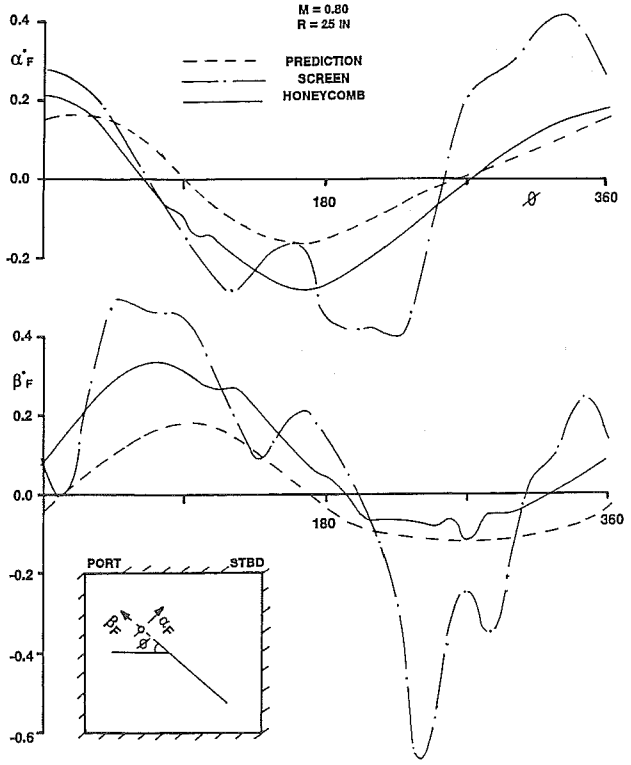

FIG 19 CIRCUMFERENTIAL VARIATION OF FLOW ANGULARITY

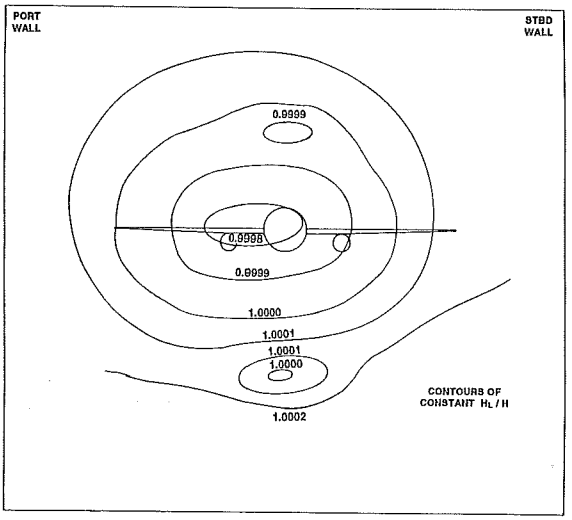

FIG 20 TUNNEL WORKING SECTION STAGNATION PRESSURE CONTOURS

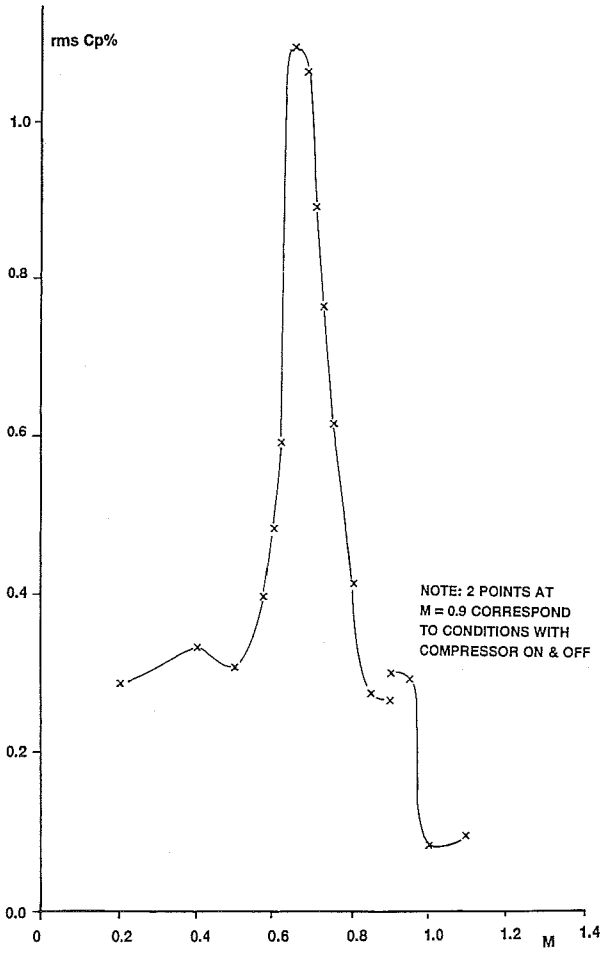

FIG 21 RMS Cp FOR MICROPHONE ON TUNNEL CENTRELINE

Preliminary analysis of hot wire measurements in the test section, at Mach numbers up to 0.5, gives a figure of 0.1% for the longitudinal turbulence level u'/U, and 0.2% for the lateral turbulence level v'/U. These figures include the unsteady velocities due to both vorticity and acoustic fluctuations and in fact the fan tones are clearly visible in the hot

wire spectra. It is appropriate to note here that, although quantitative measurements were limited to low Mach numbers, due to the non-linearity of the hot wire response above about M = 0.5, qualitative readings were obtained at Mach numbers up to 1.35, the hot wire proving robust both at high Mach numbers in the test section and at the low speed but high turbulence levels encountered in the settling chamber. The turbulence levels in the settling chamber, where the hot wire spectra are dominated by low frequencies, were found to be 1.8% and 1.0% for the longitudinal and lateral components respectively, when the test section Mach number was 0.4. The figures are slightly higher than those for measurements made at the same distance downstream of the sample of honeycomb material in the low speed tunnel, Fig 6b, but have the same relative magnitudes. Using the results of Uberoi, the measured turbulence in the settling chamber would imply test section levels of 0.11% longitudinally and 0.20% laterally. Although these values accurately match the values measured in the working section, further work will be required to confirm that the measurements are not contaminated by alternative sources such as the main fan blade passing frequency and its harmonics.

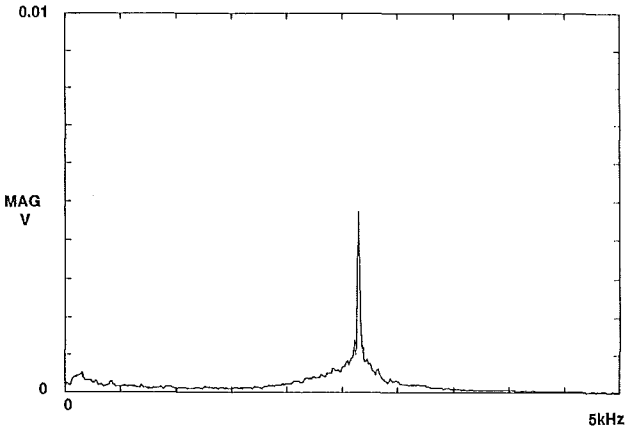

FIG 22 POWER SPECTRUM OF CENTRELINE MICROPHONE, M = 0.65

The response of the microphone mounted on the tunnel centreline is shown in Fig 21, in terms of the non-dimensionalised rms unsteady pressure. The peak value of 1.1% at M = 0.65, is considerably lower than the figure of 2.3% at M = 0.7 given in Reference 4, which it supersedes. Spectra of both the centreline and wall microphones are dominated at Mach numbers around 0.65 by a peak at about 2.6 kHz, Fig 22, with the magnitude of the peak at the wall being approximately three times that on the centre line. This peak in the spectra, which is audible as a high-pitched whistle outside the tunnel, was also remarked upon by Owen et al[5]; its cause is at present not known, though both its frequency and its relative magnitude at the wall and on the centreline suggest that it is generated by the perforated test section wall. The noise levels measured in a variety of transonic tunnels show the same trend towards a significant peak around Mach numbers of 0.6 - 0.8. During the present measurements it was found that with the traversing rig installed in the tunnel, which is a condition more relevant to model testing, the spectra show no peak around 2.6 kHz and the high peak in rms C_p disappears. Fig 23 shows a comparison of the wall microphone output with, and without, the arm present.

Detailed analysis of the unsteady microphone and hot wire data is continuing and it is hoped that it will provide a better understanding of the magnitude and the causes of the vorticity and acoustic fluctuations in the tunnel.

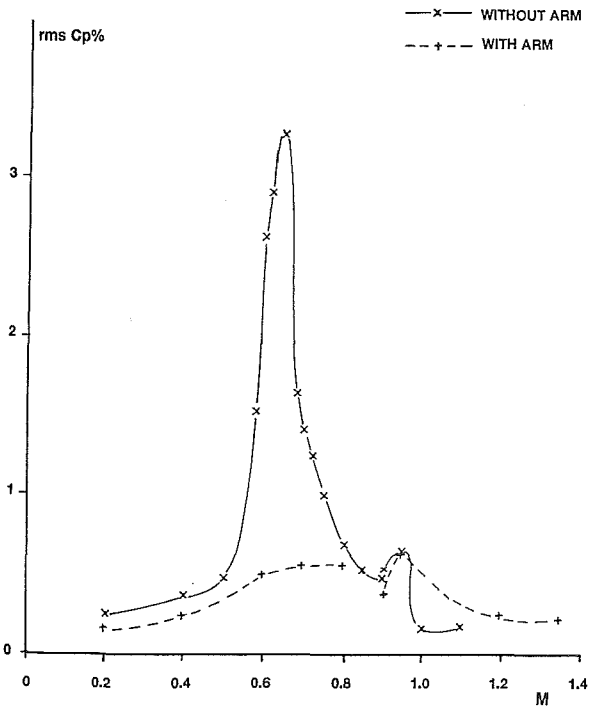

FIG 23 COMPARISON OF WALL MOUNTED MICROPHONE RESPONSE WITH & WITHOUT TRAVERSING ARM

CONCLUSIONS

A deep cell honeycomb has been installed as the sole flow smoothing device in the ARA 9' x 8' Transonic Wind Tunnel. Measurements of the flow quality have been carried out using a cruciform body to measure the flow angularity and the low frequency unsteady flow angles, a pitot rake to measure the stagnation pressure, an array of microphones and a crossed hot wire to measure unsteadiness to high frequencies. The results show that:

- the honeycomb gives a high degree of flow uniformity in the test section, consistent with a settling chamber flow which would be produced by ideal reservoir conditions.
- the low frequency unsteadiness measured by the cruciform body has been reduced to extremely low levels.
- the pitot survey of the working section can just detect the influence of the honeycomb support structure as a local reduction in H of 0.1 millibar, but this is well within the absolute accuracy of the measurement of tunnel stagnation pressure.

- measurements of static pressure fluctuations using a centreline probe show a high peak at M = 0.65 which has also been identified in previous tests with the AEDC 10° cone. This is caused by a pure tone at 2.6 kHz, which can be heard clearly outside the tunnel. Neither this tone, nor the associated peak in rms C_p, are present when the calibration rig is installed in the tunnel.

- preliminary analysis of the unsteady data yields un steady velocity components of 0.1% longitudinally and 0.2% laterally.

Further work:

- microphone measurements will be made with typical models installed in the tunnel to investigate the un steadiness relevant to actual testing. As Fig 23 indicates, 'empty' tunnel noise measurements may well be irrelevant to normal model testing, and this caveat probably applies to other tunnels besides the ARA TWT.

- detailed analysis of the extensive unsteady data will be carried out in order to construct a more complete picture of the flow unsteadiness in the test section and to identify its sources.

ACKNOWLEDGEMENTS

Development of the method of construction of the honeycomb and management and quality control of manufacture of the modules and erection of the honeycomb were the responsibility of John Day and John Carberry, supported by the Engineering Staff of ARA whose achievement in completing the project within the planned time is beyond praise. The cooperation of staff of DRA Bedford, who made available the DRA boundary layer tunnel and associated instrumentation, is also gratefully acknowledged.

REFERENCES

1 Lumley J L, McMahon J F, Reducing water tunnel turbulence by means of a honeycomb, ASME Journal of Basic Engineering, December 1967.

2 Taylor G I, Batchelor G K, The effect of wire gauze on small disturbances in a uniform stream. QuartJnl Mech & Appl Maths, V2, No 1, 1949.

3 East L F, Sawyer W G, Nash C R, An investigation of the structure of equilibrium turbulent boundary layers. RAE TR 79040, April 1979.

4 Elsenaar A, The windtunnel as a tool for laminar flow research. 17th Congress of the International Council of the Aeronautical Sciences, Vol 1, Stockholm, September 1990.

5 Owen F K, Stainback P C & Harvey W D, An evaluation of factors affecting the flow quality in wind tunnels. AGARD-CP-348, 1984.